

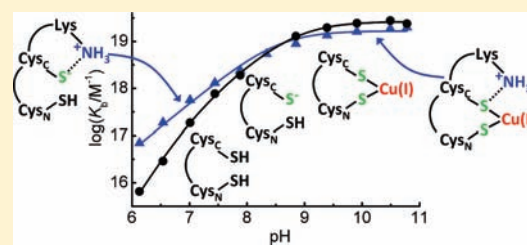
Copper Trafficking Mechanism of CXXC-Containing Domains: Insight from the pH-Dependence of Their Cu(I) Affinities

Adriana Badarau and Christopher Dennison*

Institute for Cell and Molecular Biosciences, Medical School, Newcastle University, Newcastle upon Tyne, NE2 4HH, U.K.

Supporting Information

ABSTRACT: Copper is trafficked to cellular destinations by homeostatic proteins that also prevent adverse reactivity of the metal. The copper metallochaperone HAH1 (human Atx1) binds Cu(I) via a CXXC motif on loop1/ α 1 of a $\beta\alpha\beta\beta\alpha\beta$ ferredoxin-like structure. A similar fold constitutes each of the six metal-binding domains (MBDs) of the two P-type ATPases (Menkes and Wilson disease proteins), the destination for copper bound to HAH1. In this work we have investigated the influence of pH on copper trafficking between HAH1 and the first MBD of the Menkes protein (MNK1). Cu(I) affinities of 5.6×10^{17} and $3.6 \times 10^{17} \text{ M}^{-1}$ have been determined at pH 7.0 for HAH1 and MNK1, respectively, from competition titrations with the chromophoric Cu(I) ligand bathocuproine disulfonate. The mutation of Lys60 on loop5 of HAH1 to Ala (the corresponding residue is Phe67 in MNK1) results in a 3-fold lowering of the affinity for Cu(I) at pH 7.0. The Cu(I) affinity of WT HAH1 exhibits a different pH-dependence compared to MNK1 and Lys60Ala HAH1. This arises because the pK_a of the second Cys ligand in the CXXC motif of HAH1 is 1.5 pH units lower due to stabilization of the thiolate via a hydrogen-bonding interaction with the side chain of Lys60. The thermodynamic gradient for Cu(I) transfer between HAH1 and MNK1 depends on pH. The decrease in the pK_a of the Cys ligand in HAH1 can also influence the kinetics of Cu(I) transfer.



INTRODUCTION

Copper is an essential trace element involved in key biological processes including electron transfer and oxygen metabolism. Copper has to be transported to cellular destinations without giving rise to reactive oxygen species or binding to sites for other metals.^{1–11} Copper-trafficking pathways commonly involve the metallochaperone Atx1 and copper-transporting P-type ATPases. The structures of Atx1 and the metal-binding domains (MBDs) of copper ATPases are alike, having ferredoxin-like ($\beta\alpha\beta\beta\alpha\beta$) folds. The relatively simple CXXC metal-binding motif on loop 1/ α 1 is highly conserved¹⁰ and binds a single Cu(I) ion via a two-coordinate site involving the Cys residues.^{2,5,6,10–12} A CXXC motif is also commonly found in proteins involved in disulfide oxidoreductase activity,^{13–15} where the influence of pH on reduction potential has been well characterized.¹³ Human Atx1 (HAH1) is involved in copper-dependent interactions with the six MBDs of ATP7A and ATP7B, also known as the Menkes and Wilson proteins, respectively, which can acquire copper from HAH1.¹⁶ The Cu(I) affinities of CXXC sites involved in copper homeostasis have been reported,^{17–24} but, regardless of the likely importance of Cys ligand protonation for copper affinity, little is known about the influence of pH on copper trafficking. Recently, HAH1 and the MBDs of the Menkes protein were included in a study of a number of human copper proteins, which concluded that their relative affinities for Cu(I) drive the metal to cellular destinations.²³ In humans the mishandling of copper is associated with Menkes and Wilson disease, neurodegenerative disorders, and fungal virulence.^{25–27}

A residue on loop 5 approaches the Cu(I) site in all Atx1s and MBDs. This residue is a Lys in HAH1 (Lys60), and other eukaryotic Atx1s, but is typically a Tyr in the prokaryotic proteins, although a

His is found on loop 5 in certain cyanobacterial Atx1s.²⁸ A Phe is found in the corresponding position in most of the MBDs of ATP7A/B [Phe67 in domain 1 of the Menkes protein (MNK1)] and the two MBDs of the yeast homologue Ccc2.²⁸ A range of interactions has been observed for the Lys residue on loop 5 in structures of eukaryotic Atx1s. The side chain amino group of this residue is within hydrogen-bonding distance of the S^γ of the C-terminal Cys (Cys_C, Cys15 in HAH1) of the CXXC motif in the solution structure of Cu(I)- (most models) and apo-HAH1 (some models).²⁹ In crystal structures a similar hydrogen bond is found in Atx1 (yeast),^{30,31} while in the Cu(I)-HAH1 homodimer this interaction is mediated by a water molecule.¹² This Lys residue has been implicated in the process of copper transfer to MBDs.^{11,12,28,32}

In this work we determine the Cu(I) affinities of both HAH1 and MNK1 in the pH 6 to 11 range. We also study the influence of pH on the Cu(I) affinity of the Lys60Ala HAH1 variant. In all cases Cu(I) affinities depend on pH below pH \sim 10, but in a different manner for wild type (WT) HAH1 compared to MNK1 and the Lys60Ala HAH1 variant. These effects are due to the tuning of the pK_a of one of the Cys ligands, and the data for Lys60Ala HAH1 demonstrates that the key loop 5 residue is responsible for this difference. The presence of Lys and Phe respectively in this location in HAH1 and MNK1 results in their relative affinity for Cu(I) being dependent on pH. The differing pK_a values for the Cys ligands also provide an insight into kinetic factors that drive Cu(I) transfer.

Received: October 12, 2010

Published: February 16, 2011

MATERIALS AND METHODS

Cloning and Mutagenesis. The gene coding for MNK1³³ was synthesized using a previously described method³⁴ involving two PCR steps, with some modifications. The first PCR reaction involved primers P1 to P4 (Table S1, Supporting Information) and an annealing temperature of 63 °C. The second PCR reaction used two amplification primers that included the NdeI and EcoRI restriction sites (P5 and P6 in Table S1) using an annealing temperature of 68 °C. The resulting PCR product was purified, digested, and cloned into the NdeI/EcoRI sites of pET29a to give pETMNK1. The gene coding for WT HAH1 was amplified from the plasmid pJG4.SHAH1³⁵ and cloned into the NdeI/EcoRI sites of pET29a to give pETHAH1. The Lys60Ala HAH1 variant was generated using site-directed mutagenesis (QuikChange, Stratagene) with pETHAH1 as the template and the primers K60A1 and K60A2 (Table S1). Both strands of all DNA constructs were confirmed by sequencing.

Protein Purification, Reduction, and Cu(I) Binding. *E. coli* BL21 (DE3) transformed with pETMNK1 was grown in LB media at 37 °C to an OD₆₀₀ of 1.0. Cells were induced with 1 mM isopropyl β-D-thiogalactopyranoside, harvested after 20 h, and resuspended in 25 mM tris-(hydroxymethyl)aminomethane (Tris) pH 8.5. Resolution of the crude extract by anion-exchange (Q-Sepharose FF 5 mL column, GE Healthcare) and gel filtration (Superdex 75 16/60 column, GE Healthcare) chromatography yielded apo-MNK1 (purity >95% as judged by sodium dodecyl sulfate polyacrylamide gel electrophoresis gels). The apo-protein was fully reduced by incubating overnight with 4 mM dithiothreitol (DTT), transferred to an anaerobic chamber (Belle Technology, [O₂] << 2 ppm), and desalted on a PD10 column (GE Healthcare) equilibrated and eluted with 20 mM 4-(2-hydroxyethyl)piperazine-1-ethanesulfonic acid (Hepes) pH 7.0. Cu(I)-loaded MNK1 was prepared by incubating reduced apo-protein with Cu(I) (from a 60 mM [Cu(CH₃CN)₄]PF₆ stock in acetonitrile) in 20 mM Hepes pH 7.0 plus 200 mM NaCl for 20 min. All experimental procedures involving fully reduced apo- and Cu(I)-proteins were performed under strict oxygen-free conditions, mainly in the anaerobic chamber. Similar purification, reduction, and Cu(I) loading methods were used for WT and Lys60Ala HAH1, except that cells were induced for 4 h and the cell pellet was resuspended in 25 mM Tris pH 9.5.

Determination of Protein and Copper Concentrations. The concentrations of fully reduced apo-proteins were based on the free thiol concentration determined with 5,5'-dithiobis(2-nitrobenzoic acid) (DTNB)³⁶ as described previously.³⁷ Two and three free thiols per protein molecule were considered for MNK1 and HAH1 (WT and Lys60Ala), respectively. The protein concentrations thus obtained are in good agreement with those obtained using calculated ε₂₈₀ values of 7000 and 3000 M⁻¹ cm⁻¹ for MNK1 and HAH1 (WT and Lys60Ala), respectively.³⁸ Copper concentrations were determined by atomic absorption spectroscopy (AAS) as described previously.³⁷

Circular Dichroism Spectroscopy. Far-UV circular dichroism (CD) spectra (200–250 nm) of MNK1 and HAH1 (WT and Lys60Ala) were recorded on a JASCO J-810 spectrometer at a protein concentration of 40–50 μM, in 50 mM buffer (vide infra), at 20 °C.

pH-Dependence of the Cu(I) Affinities and the Absorbance at 240 nm. The buffers used for these experiments were sodium acetate (pH 4.5–5.5), 2-(*N*-morpholino)ethanesulfonic acid (pH 5.5–6.8), Hepes (pH 6.8–7.7), *N*-tris(hydroxymethyl)methyl-3-aminopropanesulfonic acid (pH 7.7–9.0), 2-(*N*-cyclohexylamino)ethanesulfonic acid (pH 9.0–10.0), and 3-(cyclohexylamino)-1-propanesulfonic acid (Caps) (pH 10.0–11.0). Experiments were performed in 50 mM buffer, with the ionic strength (*I*) kept constant (200 mM) using NaCl, in an anaerobic cuvette (quartz; Hellma). Cu(I) affinity constants (*K_b* values) were determined using competition experiments with bathocuproine disulfonate (BCS, Aldrich, non-standardized for purity).¹⁷ These assays were monitored by the colorimetric determination (Perkin-Elmer λ35 UV/vis spectrophotometer) of the concentration of [Cu(BCS)₂]³⁻. This was measured using an extinction coefficient at 483 nm

for [Cu(BCS)₂]³⁻ determined by adding [Cu(CH₃CN)₄]PF₆ (2–20 μM) from an anaerobically prepared stock solution in a gastight syringe (Hamilton) into buffer containing 1 mM BCS, with the copper concentration verified by AAS. The value obtained (ε₄₈₃ = 12500 M⁻¹ cm⁻¹) is in good agreement with literature values of 12250–13300 M⁻¹ cm⁻¹.^{17,39} The overall association constant (*β*) of [Cu(BCS)₂]³⁻ is dependent on pH, and values were calculated using the maximum *β* value (*β*_{max}) of 6.3 × 10¹⁹ M⁻², and a p*K_a* of 5.70 for BCS¹⁷ [*β* = *β*_{max}/(1 + [H⁺]/*K_a*)²]. In a typical experiment, anaerobically prepared fully reduced (checked by DTNB assays) apo-protein (WT HAH1, Lys60Ala HAH1, and MNK1) was titrated (using a gastight syringe) into a mixture of [Cu(BCS)₂]³⁻ (15 μM) in excess BCS (10–770 μM), and the decrease in [Cu(BCS)₂]³⁻ concentration due to the formation of Cu(I)-protein was monitored from the absorbance at 483 nm. Copper affinity constants (*K_b* values) were obtained by fitting data (Origin 7) to eq 1. The titration of BCS into a mixture of Cu(I)-protein and excess apo-protein was also performed at pH 7.0 for all three proteins, and data were fit to eq 2. Below are eqs 1 and 2;

$$[P] = \frac{([Cu] - [CuL_2])([L] - 2[CuL_2])^2 \beta}{K_b [CuL_2]} + [Cu] - [CuL_2] \quad (1)$$

$$[L] = 2[CuL_2] + \sqrt{\frac{K_b([P] - [Cu] + [CuL_2])[CuL_2]}{\beta([Cu] - [CuL_2])}} \quad (2)$$

in which [L], [P], and [Cu] represent total concentrations of BCS, protein, and copper respectively.

The pH-dependence of *K_b* was fit to either a single (eq 3) or double (eq 4) ionization model, depicted in Scheme 1, and the p*K_a* values of the ionizing groups (p*K_{a1}* and p*K_{a2}*) and the affinity constant for the protein in the optimum ionization state (*K_b*^{max}) were obtained.

$$K_b = \frac{K_b^{\max}}{1 + \frac{[H^+]}{K_{a1}}} \quad (3)$$

$$K_b = \frac{K_b^{\max}}{1 + \frac{[H^+]}{K_{a1}} + \frac{[H^+]^2}{K_{a1}K_{a2}}} \quad (4)$$

To determine the p*K_a* values of Cys residues from the pH-dependence of the extinction coefficient at 240 nm (ε₂₄₀),^{40,41} fully reduced apo-proteins (15–25 μM) were prepared in 50 mM buffer (*I* = 200 mM, NaCl) in the pH range 4.5–11.0. The data were fit to eq 5, in which ε₀ is the extinction coefficient of PH₂ and Δε₂ and Δε₁ represent the difference between the extinction coefficients of PH and PH₂, and P and PH, respectively.

$$\varepsilon_{240} = \frac{\varepsilon_0 \frac{[H^+]^2}{K_{a1}K_{a2}} + (\varepsilon_0 + \Delta\varepsilon_2) \frac{[H^+]}{K_{a1}} + (\varepsilon_0 + \Delta\varepsilon_2 + \Delta\varepsilon_1)}{1 + \frac{[H^+]}{K_{a1}} + \frac{[H^+]^2}{K_{a1}K_{a2}}} \quad (5)$$

As a control, and to allow the p*K_a* of Cys41 of HAH1 to be estimated, the influence of pH on the ε₂₄₀ values of Cu(I)-HAH1 and Cu(I)-MNK1 (22 and 13 μM, respectively) was also measured in the pH range 5 to 9.5.

RESULTS AND DISCUSSION

Protein Purification. MNK1 elutes from a Superdex 75 gel filtration column at 92 mL corresponding to a molecular weight of 8.2 kDa. WT and Lys60Ala HAH1 elute from this column at 92 and 91 mL, corresponding to molecular weights of 8.2 and 8.7 kDa, respectively. The matrix-assisted laser desorption/ionization time-of-flight mass spectrum of MNK1 has peaks at 7910 and

Scheme 1

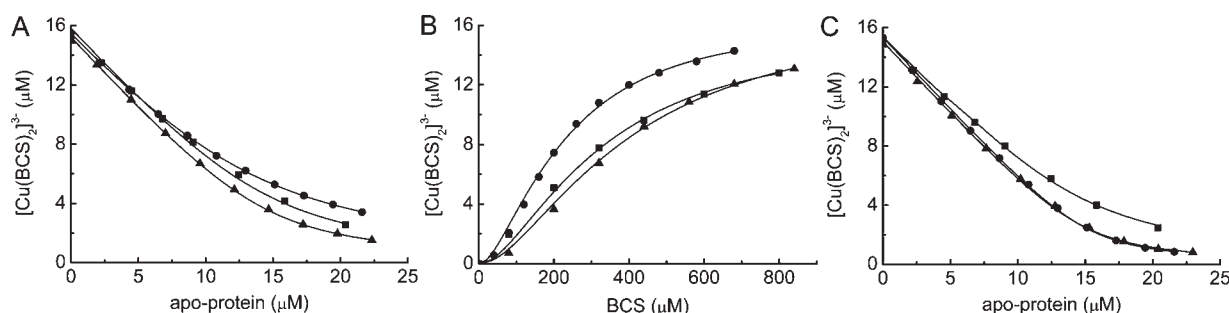
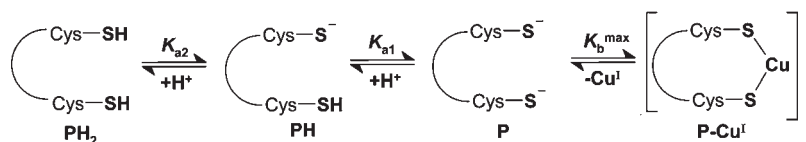


Figure 1. Cu(I) affinity determinations for WT HAH1 (\blacktriangle), Lys60Ala HAH1 (\bullet), and MNK1 (\blacksquare). (A) Titrations of apo-proteins into $[\text{Cu}(\text{BCS})_2]^{3-}$ ($15 \mu\text{M}$) and excess BCS ($70 \mu\text{M}$) in 50 mM Hepes pH 7.0 ($I = 200 \text{ mM}$, NaCl). The lines show fits of the data to eq 1, and the K_b values obtained are given in the text. (B) Titrations of BCS into Cu(I)-proteins ($16 \mu\text{M}$ for WT and Lys60Ala HAH1 and $15 \mu\text{M}$ for MNK1) and excess apo-protein (16 , 11 , and $13 \mu\text{M}$ for WT HAH1, Lys60Ala HAH1, and MNK1, respectively) in 50 mM Hepes pH 7.0 ($I = 200 \text{ mM}$, NaCl). The lines show fits of the data to eq 2 (K_b values are given in the text). (C) Titrations of apo-proteins into $[\text{Cu}(\text{BCS})_2]^{3-}$ ($15 \mu\text{M}$) and excess BCS ($370 \mu\text{M}$ for WT and Lys60Ala HAH1 and $770 \mu\text{M}$ for MNK1) in 50 mM Caps pH 10.8 ($I = 200 \text{ mM}$, NaCl), and again the lines show fits of the data to eq 1 (K_b values in the text).

8042 Da [theoretical ($- \text{Met1}$) 7910 Da, theoretical (full length) 8041 Da], whereas single peaks are observed for WT HAH1 at 7268 Da [theoretical ($- \text{Met1}$) 7271 Da] and for Lys60Ala HAH1 at 7212 Da [theoretical ($- \text{Met1}$) 7213 Da]. The far-UV CD spectra of the reduced apo-proteins are typical of folded domains and change little in the pH range studied. Apo-MNK1 is unstable at pH 5.5 and starts to precipitate.

Cu(I) Affinities and Their Dependence on pH. Titrations of fully reduced apo-proteins into a solution of $[\text{Cu}(\text{BCS})_2]^{3-}$ in the presence of an excess of BCS at pH 7.0 are shown in Figure 1A. The fits of the data to eq 1 give K_b values [Cu(I) affinity constants] of $(5.6 \pm 0.1) \times 10^{17}$, $(1.8 \pm 0.1) \times 10^{17}$, and $(3.6 \pm 0.3) \times 10^{17} \text{ M}^{-1}$ for WT HAH1, Lys60Ala HAH1, and MNK1, respectively. The titration of excess apo-protein was also performed at this pH value (Figure 1B). Data were fit to eq 2, giving K_b values of $(3.3 \pm 0.1) \times 10^{17}$, $(1.3 \pm 0.1) \times 10^{17}$, and $(2.5 \pm 0.2) \times 10^{17} \text{ M}^{-1}$, respectively, for WT HAH1, Lys60Ala HAH1, and MNK1. The Cu(I) affinities from the titrations for a particular protein in the two directions agree within 30–40%, which confirms the validity of the approach, demonstrates that the equilibrium position was reached in these titrations, and shows that no mixed BCS-Cu(I)-protein species are formed. There is considerable variability in the reported Cu(I) affinities of CXXC-containing copper trafficking proteins (Table 1). These differences are too large in most cases to be due to alterations in the pH values of these determinations (vide infra) and are much more dependent on the measurement method (this issue has recently been discussed in detail²⁴). The direct titration of Cu(I) into protein, analyzed by isothermal titration calorimetry, provides much lower affinity constants for a range of reasons.²⁴ The differences observed with competing Cu(I) ligands are primarily due to uncertainties in the Cu(I) affinities of some of these ligands. For example, the β value for the complex between Cu(I) and bicinchoninic acid determined in

Table 1. Cu(I) Affinities of Atx1s and MBDs

protein (organism)	K_b (M^{-1}) (pH)
HAH1 (<i>Homo sapiens</i>)	5.6×10^{17} (7.0) ^{a,b}
	2.6×10^{17} (7.0) ^{b,24}
	6.0×10^{13} (7.5) ^{c,23}
	3.5×10^{10} (7.5) ^{d,19}
	2.5×10^5 (6.5) ^{e,18}
Lys60Ala HAH1 (<i>H. sapiens</i>)	1.8×10^{17} (7.0) ^{a,b}
	3.6×10^{17} (7.0) ^{a,b}
MNK1 (<i>H. sapiens</i>)	4.0×10^{14} (7.5) ^{c,23}
	$7.7 \times 10^{13} - 3.8 \times 10^{14}$ (7.5) ^{c,23}
MNK2, 5, and 6 (<i>H. sapiens</i>)	9.6×10^{12} (7.5) ^{c,23}
Wilson protein MBDs 1–6 (<i>H. sapiens</i>)	$2.2 \times 10^{10} - 6.3 \times 10^{10}$ (7.5) ^{d,19}
	$2.1 \times 10^5 - 4.7 \times 10^6$ (6.5) ^{e,18}
	$1.4 \times 10^{18} - 2.4 \times 10^{18}$ (8.0) ^{b,17}
Atx1 (<i>Saccharomyces cerevisiae</i>)	10^{16} (6.0) ^{b,21}
Ccc2a ^f (<i>S. cerevisiae</i>)	$6.3 \times 10^{18} - 7.1 \times 10^{18}$ (8.0) ^{b,17}
CopZ ^g (<i>Bacillus subtilis</i>)	$\sim 10^{17}$ (7.5) ^{b,20}
CopZ ^g (<i>Archaeoglobus fulgidus</i>)	6.6×10^{14} (7.5) ^{d,h,22}
CopA ⁱ (<i>A. fulgidus</i>)	$> 10^{14}$ (7.5) ^{d,h,22}
	6.8×10^{11} (7.5) ^{d,j,22}

^a Values obtained in the present study from titrations of apo-proteins into $[\text{Cu}(\text{BCS})_2]^{3-}$. Data obtained from competition titrations with ^b BCS, ^c DTT, and ^d bicinchoninic acid. ^e In some cases, values have been obtained from the direct titration of copper monitored by isothermal titration calorimetry. ^f The first MBD of Ccc2. ^g Bacterial Atx1. ^h For the C-terminal domain. ⁱ Bacterial P-type ATPase. ^j For the N-terminal domain.

two separate studies differs by approximately 2–3 orders of magnitude.^{19,24} For the studies using DTT as the competing ligand, only the 1:1 Cu(I)–DTT complex⁴² was considered, thus underestimating the Cu(I) affinities, which have been referred to as apparent rather than absolute values.²³

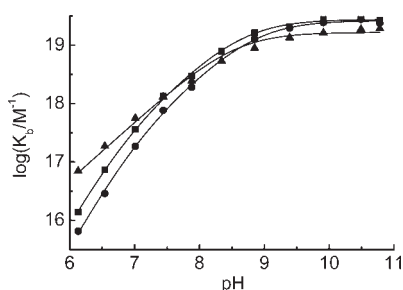


Figure 2. Plots of $\log K_b$ against pH for WT HAH1 (\blacktriangle), Lys60Ala HAH1 (\bullet), and MNK1 (\blacksquare). The lines show fits of the data to eq 3 for WT HAH1 and eq 4 for Lys60Ala HAH1 and MNK1, giving the pK_a and K_b^{\max} values listed in Table 2.

Table 2. Maximum Cu(I) Affinity Constants (K_b^{\max}), pK_a , and $\Delta\epsilon_{240}$ values for WT HAH1, Lys60Ala HAH1, and MNK1^a

	WT HAH1	Lys60Ala HAH1	MNK1
$K_b^{\max} \times 10^{-19} (M^{-1})$	1.7 ± 0.1	2.6 ± 0.1	2.8 ± 0.1
$pK_{a1} (K_b)$	8.5 ± 0.1	8.9 ± 0.1	8.7 ± 0.1
$pK_{a1} (\epsilon_{240})$	8.9 ± 0.1	8.9 ± 0.1	9.2 ± 0.2
$pK_{a2} (K_b)$	<6	6.9 ± 0.1	6.7 ± 0.1
$pK_{a2} (\epsilon_{240})$	5.5 ± 0.1	7.0 ± 0.2	7.0 ± 0.1
$\Delta\epsilon_1 (mM^{-1} cm^{-1})$	7.9 ± 0.5	7.7 ± 0.5	4.0 ± 0.6
$\Delta\epsilon_2 (mM^{-1} cm^{-1})$	3.6 ± 0.2	3.6 ± 0.4	3.3 ± 0.2

^a Subscripts 1 and 2 refer to Cys_N (Cys12 in HAH1 and Cys15 in MNK1) and Cys_C (Cys15 in HAH1 and Cys18 in MNK1), respectively.

The K_b values measured for WT HAH1, Lys60Ala HAH1, and MNK1 at pH 10.8 are $(2.0 \pm 0.1) \times 10^{19}$, $(2.4 \pm 0.1) \times 10^{19}$, and $(2.7 \pm 0.2) \times 10^{19} M^{-1}$, respectively (Figure 1C). The Cu(I) affinities for the three proteins are dependent on pH, and values have been measured in the pH range 10.8 to 6.1 (Figure 2) from titrations of apo-proteins into $[Cu(BCS)_2]^{3-}$ (data could not be compared at lower pH values because of the instability of MNK1). A sigmoidal dependence on pH is seen in all cases, and for WT HAH1 there is a first-order increase in Cu(I) affinity with decreasing $[H^+]$ from pH 6.1 to 9.0, followed by a plateau (Figure 2). This indicates that the deprotonation of a single residue influences affinity in this pH range. The data were fit to a single ionization model (eq 3), which yielded a K_b^{\max} of $(1.7 \pm 0.1) \times 10^{19}$ and a pK_a (pK_{a1}) of 8.5 ± 0.1 (Table 2), typical for a Cys residue in aqueous solution.⁴³ This is consistent with this pK_a arising from the N-terminal Cys (Cys_N, Cys12 in HAH1, vide infra) which is solvent exposed in the solution structure of apo-HAH1.²⁹ Lys60Ala HAH1 and MNK1 also show a first-order increase in K_b with decreasing $[H^+]$ in the pH 7.5 to 9.0 region, followed by a plateau at higher pH, but below pH 7.5 the slope of the $\log K_b$ versus pH plot is greater than 1. These data fit a model where two ionizing groups influence Cu(I) binding (eq 4), with pK_a values (pK_{a1} and pK_{a2} , respectively) of 8.9 ± 0.1 and 6.9 ± 0.1 for Lys60Ala HAH1 and 8.7 ± 0.1 and 6.7 ± 0.1 for MNK1 (Table 2).

Determination of the pK_a Values of the Cys Ligands from the Absorbance at 240 nm. MNK1 possesses only the two Cys residues in the CXXC motif, while HAH1 has an additional Cys (Cys41) that is not involved in metal binding, as it is $>17 \text{ \AA}$ from the CXXC motif.¹² This is consistent with the rapid reaction of all three Cys residues of apo-HAH1 with DTNB, while in the Cu(I)-protein only one Cys exhibits fast reactivity (Figure S1, Supporting Information). Both HAH1 and MNK1 possess Tyr residues,

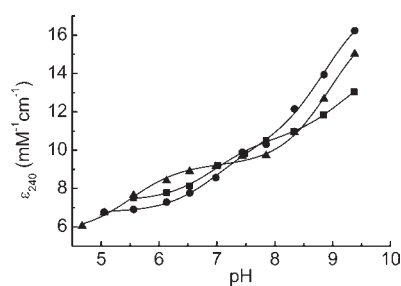


Figure 3. Plot of ϵ_{240} against pH for WT HAH1 (\blacktriangle), Lys60Ala HAH1 (\bullet), and MNK1 (\blacksquare). The lines show fits of the data to eq 5 and give the pK_a and $\Delta\epsilon$ values shown in Table 2.

which also absorb at 240 nm, and complicate the analysis of these data at higher pH values (a band at 293 nm, corresponding to tyrosine phenolate⁴⁴ appears above pH ~ 9.5). Therefore, only data below pH 9.5 were considered in the analysis of the pH dependence of ϵ_{240} . The data were fit to a two-ionization model (eq 5), giving a low and a high pK_a (pK_{a2} and pK_{a1} , respectively) in all cases (Figure 3 and Table 2). The pK_{a2} values are in good agreement with those found from Cu(I) affinity measurements for Lys60Ala HAH1 and MNK1. For WT HAH1, pK_{a2} is outside of the pH range in which K_b was measured ($pK_{a2} < 6.1$). There is a greater error in pK_{a1} and the associated extinction coefficient change ($\Delta\epsilon_1$), as a plateau in absorbance is not reached up to pH 9.5. Therefore, the pK_{a1} values determined from the Cu(I) affinity measurements are more reliable, although the agreement is good between the values determined using the two approaches (Table 2). The $\Delta\epsilon_1$ values for WT and Lys60Ala HAH1 are both approximately twice that for MNK1 (Table 2), which indicates that Cys41 of HAH1 also ionizes in this pH range. This is confirmed by comparison of the influence of pH on ϵ_{240} for Cu(I)-HAH1 and Cu(I)-MNK1, as a sizable increase is only observed in the former above pH 8 (Figure S2, Supporting Information). From these data the pK_a for Cys41 in HAH1 is ~ 9 (assuming a $\Delta\epsilon_{240}$ of $4 mM^{-1} cm^{-1}$, Table 2), but interference from Tyr residues in this pH range (vide supra) prevents a more precise determination. The Cu(I)-HAH1 data have been used to correct the ϵ_{240} data for the apo-protein above pH 8.0, and a fit to eq 5 gives pK_{a1} (ϵ_{240}) and $\Delta\epsilon_1$ values of 8.7 ± 0.1 [giving even better agreement with the pK_{a1} (K_b) value] and $4.1 \pm 0.3 mM^{-1} cm^{-1}$ respectively (Figure S3, Supporting Information).

Insight into Copper Trafficking from the pK_a s of the Cys Ligands. pK_a values of 9.2 and 5.5 were previously reported for the Cys residues in the CXXC motif of the Atx1-like mercury detoxifying protein MerP.⁴⁵ These were assigned to the Cys_N and Cys_C residues, respectively, and we favor the same assignment for pK_{a1} and pK_{a2} in both HAH1 and MNK1. Our studies demonstrate that a major contributing factor to the lower pK_{a2} for Cys15 (Cys_C) in HAH1 is the presence of Lys60, as the value is raised by 1.5 pH units in the Lys60Ala variant to match that found for MNK1 (Table 2). An interaction (purely electrostatic or hydrogen bonding) between the side chains of Lys60 and Cys15 stabilizes the thiolate in HAH1 and lowers the pK_a (Figure 4). Although conformational variability is observed for Lys60 in solution structures of apo- and Cu(I)-HAH1, relatively short distances ($\sim 3.0\text{--}3.5 \text{ \AA}$) are found between the N⁵ and S⁷ atoms,²⁹ as is also the case in the complex with MNK1 (Figure 4B).³³ Tyr62 in the same position of the MBD of the mercuric ion reductase MerA has recently been proposed to alter the coordinating Cys pK_a .⁴⁴ Furthermore, His61, in the corresponding position on loop 5 of the Atx1 from *Synechocystis*

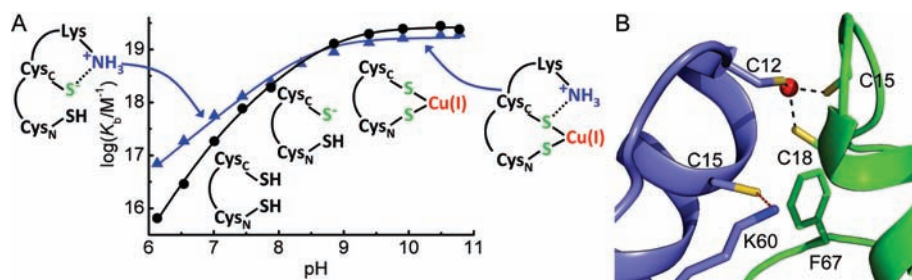


Figure 4. (A) Plots of $\log K_b$ against pH for WT HAH1 (\blacktriangle , in blue) and Lys60Ala HAH1 (\bullet) including schematic representations of the forms of the CXXC motifs present in the different pH ranges. (B) The arrangement found in model 3 of the solution complex of HAH1 (slate) and MNK1 (green). The side chains of the two Cys ligands and the residue on loop 5 are shown as stick representations with the copper ion as a red sphere and the hydrogen bond between the N^ε atom of Lys60 and the S^γ of Cys15 shown as a dashed red line.

PCC6803, lowers the pK_a of Cys_C by ~ 1 pH unit (A. Badarau and C. Dennison, unpublished data). A residue on loop 5 that can form a hydrogen bond with Cys_C appears to result in the lowering of the pK_a of this ligand. The presence of a Phe on loop 5 in the MBDs of the ATPases, such as in MNK1, which cannot make this interaction, results in Cys_C of their CXXC motifs having a much higher pK_a (Figure 4). In these domains, Cys_C still has a lower pK_a than that of Cys_N (as is also the case in the Lys60Ala HAH1 variant) which could be partly due to Cys_C being located toward the N-terminus of $\alpha 1$.⁴⁵

The maximum Cu(I) affinity (K_b^{\max}) is 2-fold lower for WT HAH1 than for MNK1 (Table 2). The affinities are very similar in the pH 7.0–8.0 range, but the MNK1 Cu(I) affinity is ~ 5 -fold lower at pH 6.1 (Figure 2). The thermodynamic gradient for Cu(I) transfer between Atx1 (yeast) and the first MBD of Ccc2 (Ccc2a) has been found to be shallow.^{5,17,46} Herein we show that the gradient for Cu(I)-trafficking from HAH1 to the MBD changes from being shallow at alkaline and neutral pH, to much more steep and unfavorable below pH 7. The pH of the cytosol of a human cell is typically 7.0–7.4.⁴⁷ However, apoptosis is associated with acidification of the cytosol to values as low as pH 5.8,⁴⁸ and several diseases where apoptosis is dysregulated, such as cancer and neurological disorders, are linked to copper imbalance.^{26,27,49} The importance of pH when comparing Cu(I) affinities of proteins is evident, even for those sharing the same fold and metal binding motif. The thiolate nucleophilicity series predicted from our pK_a determinations is Cys_N (HAH1/Atx1) \sim Cys_N (MBD) $>$ Cys_C (MBD) $>$ Cys_C (HAH1/Atx1).⁵⁰ This series is consistent with the solution structure of the HAH1-MNK1 complex in the presence of copper,³³ in which Cys_C of HAH1 is not involved in coordinating Cu(I), indicating that it has lower nucleophilicity than that of the other three Cys ligands (Figure 4B). NMR studies of Atx1 (yeast) and Ccc2a (MBD) are more revealing and again, consistent with our nucleophilicity series, show that Cys_N from both proteins are essential for complex formation, with Cys_C of Ccc2a being the preferred third Cu(I) ligand in the complex.⁵¹

As well as affecting the thermodynamics of Cu(I) transfer, the acidity of the Cys ligands can influence the rate of Cu(I) exchange. Computational studies have shown that the rate-determining step in the Cu(I) transfer reaction between two CXXC motifs is the rearrangement of a three-coordinate intermediate from a more reactant-like form, where both Cys_N and Cys_C of the donor are Cu(I) ligands, to a more product-like species at which both Cys_N and Cys_C of the acceptor are ligands.⁵² This occurs via the concerted attack of Cys_C of the acceptor and dissociation of Cys_C of the donor. This reaction will be favored by a more nucleophilic Cys_C (higher pK_a) in the acceptor, and a better leaving group Cys_C (lower pK_a) in the donor. The pK_a values of these nonligating

thiols in the two possible three-coordinate intermediates may differ from those determined for the apo-proteins. However, Lys60 will still increase the acidity of Cys_C in HAH1, making it a better leaving group. Interestingly, the pK_a of Cys_C in MNK1 offers a good compromise between a high thiolate concentration (70–85% at pH 7.4) and optimized nucleophilicity. It thus appears that eukaryotes have evolved to lower the activation barrier for Cu(I) transfer from the metallochaperone to the target MBD, by employing Lys and Phe, respectively, on loop 5 in the vicinity of Cys_C. Moreover, the activation energy of the reaction in the opposite direction, i.e., Cu(I) transfer from the MBD to the chaperone, is increased, for the same reason, which ensures vectorial Cu(I) transfer.

CONCLUSIONS

In this study we demonstrate that the thermodynamics of Cu(I) transfer from HAH1 to a target domain of the Cu(I) transporter ATP7A (MNK1) are dependent on pH and become less favorable as the pH is decreased below 7.0. This is caused by a decrease in the pK_a of the second Cys ligand (Cys_C) of the Cu(I)-binding motif of HAH1, because of an interaction, probably a hydrogen bond, with a conserved Lys on loop 5 (Lys60). The resulting decrease in nucleophilicity of this Cys facilitates Cu(I) release to the target MBD. These data highlight that one advantage of using Cys rather than Met⁵³ ligands in Cu(I) trafficking sites is that their Cu(I) affinity and reactivity can be controlled by modulating the pK_a . In most prokaryotes, both the Atx1 and the target MBDs have a Tyr on loop 5 in place of Lys60. We would imagine that this residue will lower the pK_a of Cys_C in both proteins, which could explain the solely regulatory role proposed for MBDs in a prokaryotic system,²² compared to eukaryotic MBDs which are involved in both Cu(I) transfer and regulation.^{16,54,55}

ASSOCIATED CONTENT

Supporting Information. A table listing the primers used and figures showing the reaction of apo- and Cu(I)-HAH1 with DTNB, the influence of pH on the ϵ_{240} of Cu(I)-HAH1 and Cu(I)-MNK1, and an alternative fit of the pH dependence of the ϵ_{240} of apo-HAH1 to eq 5. This material is available free of charge via the Internet at <http://pubs.acs.org>.

AUTHOR INFORMATION

Corresponding Author

christopher.dennison@ncl.ac.uk

ACKNOWLEDGMENT

This work was supported by BBSRC (grant BB/E016529). We thank GlaxoSmithKline for the plasmid from which HAH1 was cloned.

REFERENCES

- (1) Odermatt, A.; Solioz, M. *J. Biol. Chem.* **1995**, *270*, 4349–4354.
- (2) Pufahl, R. A.; Singer, C. P.; Peariso, K. L.; Lin, S. J.; Schmidt, P. J.; Fahrni, C. J.; Culotta, V. C.; Penner-Hahn, J. E.; O'Halloran, T. V. *Science* **1997**, *278*, 853–856.
- (3) Valentine, J. S.; Gralla, E. B. *Science* **1997**, *278*, 817–818.
- (4) Rae, T. D.; Schmidt, P. J.; Pufahl, R. A.; Culotta, V. C.; O'Halloran, T. V. *Science* **1999**, *284*, 805–808.
- (5) Huffman, D. L.; O'Halloran, T. V. *Annu. Rev. Biochem.* **2001**, *70*, 677–701.
- (6) Finney, L. A.; O'Halloran, T. V. *Science* **2003**, *300*, 931–936.
- (7) Carr, H. S.; Winge, D. R. *Acc. Chem. Res.* **2003**, *36*, 309–316.
- (8) Tottley, S.; Waldron, K. J.; Firbank, S. J.; Reale, B.; Bessant, C.; Sato, K.; Cheek, T. R.; Gray, J.; Banfield, M. J.; Dennison, C.; Robinson, N. J. *Nature* **2008**, *455*, 1138–1142.
- (9) Macomber, L.; Imlay, J. A. *Proc. Natl. Acad. Sci. U.S.A.* **2009**, *106*, 8344–8349.
- (10) Boal, A. K.; Rosenzweig, A. C. *Chem. Rev.* **2009**, *109*, 4760–4779.
- (11) Robinson, N. J.; Winge, D. R. *Annu. Rev. Biochem.* **2010**, *79*, 1–26.
- (12) Wernimont, A. K.; Huffman, D. L.; Lamb, A. L.; O'Halloran, T. V.; Rosenzweig, A. C. *Nat. Struct. Biol.* **2000**, *7*, 766–771.
- (13) Chivers, P. T.; Prehoda, K. E.; Raines, R. T. *Biochemistry* **1997**, *36*, 4061–4066.
- (14) Fomenko, D. E.; Gladyshev, V. N. *Biochemistry* **2003**, *42*, 11214–11225.
- (15) Lewin, A.; Crow, A.; Hodson, C. T. C.; Hederstedt, L.; Le Brun, N. E. *Biochem. J.* **2008**, *414*, 81–91.
- (16) Kaplan, J. H.; Lutsenko, S. *J. Biol. Chem.* **2009**, *284*, 25461–25465.
- (17) Xiao, Z.; Loughlin, F.; George, G. N.; Howlett, G. J.; Wedd, A. G. *J. Am. Chem. Soc.* **2004**, *126*, 3081–3090.
- (18) Wernimont, A. K.; Yatsunyk, L. A.; Rosenzweig, A. C. *J. Biol. Chem.* **2004**, *279*, 12269–12276.
- (19) Yatsunyk, L. A.; Rosenzweig, A. C. *J. Biol. Chem.* **2007**, *282*, 8622–8631.
- (20) Zhou, L.; Singleton, C.; Le Brun, N. *Biochem. J.* **2008**, *413*, 459–465.
- (21) Miras, R.; Morin, I.; Jacquin, O.; Cuillel, M.; Guillain, F.; Mintz, E. *J. Biol. Inorg. Chem.* **2008**, *13*, 195–205.
- (22) González-Guerrero, M.; Argüello, J. M. *Proc. Natl. Acad. Sci. U.S.A.* **2008**, *105*, 5992–5997.
- (23) Banci, L.; Bertini, I.; Ciofi-Baffoni, S.; Kozyreva, T.; Zovo, K.; Palumaa, P. *Nature* **2010**, *465*, 645–648.
- (24) Xiao, Z.; Wedd, A. G. *Nat. Prod. Rep.* **2010**, *27*, 768–789.
- (25) Bush, A. I. *Curr. Opin. Chem. Biol.* **2000**, *4*, 184–191.
- (26) Madsen, E.; Gitlin, J. D. *Annu. Rev. Neurosci.* **2007**, *30*, 317–337.
- (27) Kim, B. E.; Nevitt, T.; Thiele, D. J. *Nat. Chem. Biol.* **2008**, *4*, 176–185.
- (28) Arnesano, F.; Banci, L.; Bertini, I.; Ciofi-Baffoni, S.; Molteni, E.; Huffman, D. L.; O'Halloran, T. V. *Genome Res.* **2002**, *12*, 255–271.
- (29) Anastassopoulou, I.; Banci, L.; Bertini, I.; Cantini, F.; Katsari, E.; Rosato, A. *Biochemistry* **2004**, *43*, 13046–13053.
- (30) Alvarez, H. M.; Xue, Y.; Robinson, C. D.; Canalizo-Hernández, M. A.; Marvin, R. G.; Kelly, R. A.; Mondragon, A.; Penner-Hahn, J. E.; O'Halloran, T. V. *Science* **2009**, *327*, 331–334.
- (31) Rosenzweig, A. C.; Huffman, D. L.; Hou, M. Y.; Wernimont, A. K.; Pufahl, R. A.; O'Halloran, T. V. *Structure* **1999**, *7*, 605–617.
- (32) Hussain, F.; Rodriguez-Granillo, A.; Wittung-Stafshede, P. *J. Am. Chem. Soc.* **2009**, *131*, 16371–16373.
- (33) Banci, L.; Bertini, I.; Calderone, V.; Della-Malva, N.; Felli, I. C.; Neri, S.; Pavelkova, A.; Rosato, A. *Biochem. J.* **2009**, *422*, 37–42.
- (34) Harrison, M. D.; Dennison, C. *Proteins* **2004**, *55*, 426–435.
- (35) B. Angeletti, B.; Waldron, K. J.; Freeman, K. B.; Bawagan, H.; Hussain, I.; Miller, C. C. J.; Lau, K. F.; Tennant, M. E.; Dennison, C.; Robinson, N. J.; Dingwall, C. *J. Biol. Chem.* **2005**, *280*, 17930–17937.
- (36) Ellman, G. L. *Arch. Biochem. Biophys.* **1959**, *82*, 70–77.
- (37) Badarau, A.; Firbank, S. J.; McCarthy, A. A.; Banfield, M. J.; Dennison, C. *Biochemistry* **2010**, *49*, 7798–7810.
- (38) Gasteiger, E.; Hoogland, C.; Gattiker, A.; Duvaud, S.; Wilkins, M. R.; Appel, R. D.; Bairoch, A. In *The Proteomics Protocols Handbook*; Walker, J. M., Ed.; Humana Press Inc.: Totowa, NJ, 2005; pp 571–607.
- (39) Blair, D.; Diehl, H. *Talanta* **1961**, *7*, 163–174.
- (40) Polgar, L. *FEBS Lett.* **1974**, *38*, 187–190.
- (41) Witt, A. C.; Lakshminarasimhan, M.; Remington, B. C.; Hasim, S.; Pozharski, E.; Wilson, M. A. *Biochemistry* **2008**, *47*, 7430–7440.
- (42) Krezel, A.; Lesniak, W.; Jezowska-Bojczuk, M.; Mlynarz, P.; Brasun, J.; Kozlowski, H.; Bal, W. *J. Inorg. Biochem.* **2001**, *84*, 77–88.
- (43) Thurlkill, R. L.; Grimsley, G. R.; Scholtz, J. M.; Pace, C. N. *Protein Sci.* **2006**, *15*, 1214–1218.
- (44) Ledwidge, R. L.; Hong, B.; Miller, S. M. *Biochemistry* **2010**, *49*, 8988–8998.
- (45) Powlowski, J.; Sahlman, L. *J. Biol. Chem.* **1999**, *274*, 33320–33326.
- (46) Huffman, D. L.; O'Halloran, T. V. *J. Biol. Chem.* **2000**, *275*, 18611–18614.
- (47) Bright, G. R.; Fisher, G. W.; Rogowska, J.; Taylor, D. L. *J. Cell Biol.* **1987**, *104*, 1919–1933.
- (48) Nilsson, C.; Kagedal, K.; Johansson, U.; Ollinger, K. *Methods Cell Sci.* **2003**, *25*, 185–194.
- (49) Turski, M. L.; Thiele, D. J. *J. Biol. Chem.* **2009**, *284*, 717–721.
- (50) Basolo, F.; Johnson, R. C. *Coordination Chemistry*; Science Reviews: Wilmington, DE, 1986.
- (51) Banci, L.; Bertini, I.; Cantini, F.; Felli, I. C.; Gonnelli, L.; Hadjilias, N.; Pierattelli, R.; Rosato, A.; Voulgaris, P. *Nat. Chem. Biol.* **2006**, *2*, 367–368.
- (52) Rodriguez-Granillo, A.; Crespo, A.; Estrin, D. A.; Wittung-Stafshede, P. *J. Phys. Chem. B* **2010**, *114*, 3698–3706.
- (53) Davis, A. V.; O'Halloran, T. V. *Nat. Chem. Biol.* **2008**, *4*, 148–151.
- (54) Lutsenko, S.; LeShane, E. S.; Shinde, U. *Arch. Biochem. Biophys.* **2007**, *463*, 134–148.
- (55) Morin, I.; Gudim, S.; Mintz, E.; Cuillel, M. *FEBS J.* **2009**, *276*, 4483–4495.